Ci 11
(300/1961)

UDC 531.787 : 624.131.5

ACTA POLYTECHNICA SCANDINAVICA

CIVIL ENGINEERING AND BUILDING CONSTRUCTION SERIES No. 11

Vagn Askegaard

Measurement of Pressure between a Rigid Wall and a Compressible Medium by Means of Pressure Cells

Danish Contribution No. 14
COPENHAGEN 1961

ACTA POLYTECHNICA SCANDINAVICA

... a Scandinavian contribution to international engineering sciences

Published under the auspices of the Scandinavian Council for Applied Research

in *Denmark* by the Danish Academy of Technical Sciences

in *Finland* by the Finnish Academy of Technical Sciences, the Swedish Academy of Engineering Sciences i Finland, and the State Institute for Technical Research

in *Norway* by the Norwegian Academy of Technical Science and the Royal Norwegian Council for Scientific and Industrial Research

in *Sweden* by the Royal Swedish Academy of Engineering Sciences, the Swedish Natural Science Research Council, and the Swedish Technical Research Council

Acta Polytechnica Scandinavica consists of the following sub-series:
Chemistry including Metallurgy Series, Ch
Civil Engineering and Building Construction Series, Ci
Electrical Engineering Series, El
Mathematics and Computing Machinery Series, Ma
Mechanical Engineering Series, Me
Physics including Nucleonics Series, Ph

For subscription to the complete series or to one or more of the sub-series and for purchase af single copies, please write to

ACTA POLYTECHNICA SCANDINAVICA PUBLISHING OFFICE
Box 5073
Stockholm 5 Phone 61 47 53

This issue is published by
THE DANISH ACADEMY OF TECHNICAL SCIENCES
Copenhagen, Denmark

UDC. 531.787:624.131.5

MEASUREMENT OF PRESSURE BETWEEN A RIGID WALL AND A COMPRESSIBLE MEDIUM BY MEANS OF PRESSURE CELLS

BASIC CONSIDERATIONS CONCERNING THREE TYPES OF PRESSURE CELLS

VAGN ASKEGAARD

Structural Research Laboratory

Technical University of Denmark

ACTA POLYTECHNICA SCANDINAVICA

Civil Engineering and Building Construction Series No. 11

AP 300/1961

SUMMARY

Three types of pressure cells are assessed. The relation between the deflexion of the front plate and the error in registration of the pressure cell is given as a function of the dimensions of the pressure cell and the physical constants for the cell and for the compressible medium. The latter is assumed to be homogeneous and isotropic and to follow Hooke's law.

The following types of pressure distribution between the pressure cell and the compressible medium are considered: uniformly distributed pressure, axially symmetrical pressure distribution, and arbitrary pressure distribution. These pressure distributions refer to the imaginary state in which the deflexions of the front plate are 0 everywhere.

F. L. Smidth & Co. A/S's Jubilæumsfond has kindly granted financial support for the work described in the present paper.

MEASUREMENT OF PRESSURE BETWEEN A RIGID WALL AND A COMPRESSIBLE MEDIUM BY MEANS OF PRESSURE CELLS

BASIC CONSIDERATIONS CONCERNING THREE TYPES OF PRESSURE CELLS

Vagn Askegaard
Structural Research Laboratory
Technical University of Denmark

In this article an appraisal is made of three types of pressure cells placed in a rigid wall or plate. The front plates of the cells lie flush with the plane underside of the wall, which is, in turn, in contact with a compressible medium. Such pressure cells are used to obtain correct measurement of the pressure between the rigid wall and the compressible medium at the location of the pressure cell. The dimensions of plate and compressible medium are large in relation to the diameter of the cells.

The following cases are considered:

1. Uniformly distributed pressure under the pressure cell.
2. Axially symmetrical pressure distribution under the pressure cell.
3. Arbitrary pressure distribution under the pressure cell.
4. The pressure cell arranged in the rigid wall so that it lies near the edge or corner of this.
5. Model tests corresponding to a combination of 3. and 4.

Points 2. and 3. are included because experience shows that quite considerable pressure gradients may arise between a rigid wall and a compressible medium over an area of the same size that covered by a pressure cell.

The following assumptions are made unless otherwise stated.

A) The wall is infinitely rigid.

B) The compressible medium is isotropic and homogeneous and is subject to Hooke's law.

C) There is no friction between the compressible medium and the rigid wall plus pressure cell.

D) Tensile stresses cannot be transferred between the compressible medium and the rigid wall plus pressure cell.

The three different types of pressure cells are shown in figs. 1, 2 and 3. They are all axially symmetrical, with radius a. Pressure cells of these types are known to be used in practice.

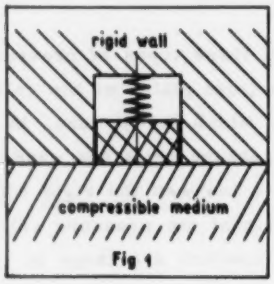

Fig 1

Fig. 1 (pressure cell a) shows a type of cell in which the front plate is rigid and moves as a frictionless piston in a cylindrical boring with radius a. The total load under the piston is equal to the spring force measured. The practical design of such a pressure cell naturally deviates considerably from that sketched.

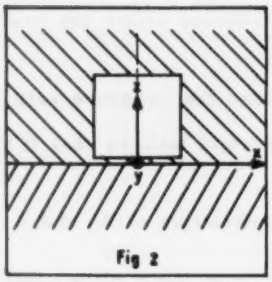

Fig 2

Fig. 2 (pressure cell b) shows a pressure cell in which the front plate is clamped along the edge. In case of pressure distribution under the front plate, this is deformed, and a relationship is sought between the resultant load under the plate and this maximum or average deflexion. In the design shown in fig. 7, the load on the plate is transferred through a fluid to a thin plate of smaller diameter. The deformation of this thin plate is measured and used as an expression of the total pressure under the front plate

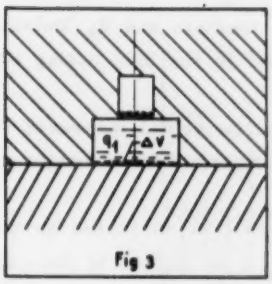

Fig 3

The pressure cell shown in fig. 3 (pressure cell c) is provided with a membrane, which transfers the pressure to a fluid. This in turn deforms a thin plate having a considerably smaller radius, and the deformation of the thin plate is then determined.

Uniformly distributed pressure under the pressure cell

It is assumed that there is pressure everywhere between the rigid wall and the compressible medium. Under the cell this pressure is uniformly distributed q_o when the front plate of the cell lies flush with the underside of the rigid wall, i.e. when $w_r = 0$, w_r being the deflexion of the front plate at a distance r from its centre.

$P = \pi a^2 q_o$ is the load that the pressure cell should register if working correctly. As the measuring operation is conditioned by whether or not w has a finite value, and as this results in a rearrangement of the pressure distribution under the cell, the force acting on the cell (and registered by this) is no longer $P = \pi a^2 q_o$, but $P - \Delta P$.

The derivative $\frac{dP}{dw}$ for $w = 0$ seems thus to characterize an important property of the pressure cell. ΔP depends on the design of the cell and on the material constants in the cell and in the compressible medium. An effort is made to design the pressure cell in such a way that ΔP is so small in relation to P (e.g. $< 0.01 - 0.02\ P$) that a correction is no longer considered necessary. On the basis of the results in (1) and (2) it can be assumed with good approximation that for $\Delta P < 0.1 \cdot P$, $\frac{\Delta P}{\Delta w} = \text{const.} = \frac{dP}{dw}_{w=0}$.

Pressure cell a (fig. 1)

According to (1) and (2), $\frac{dP}{dw}_{w=0} = 6.1\frac{E_B a}{1-\nu_B^2}$, where E_B is the modulus of elasticity of the compressible medium and ν_B Poisson's ratio. The signal measured is proportional to the load acting on the pressure cell.

The relationship between the load and the signal measured can be determined in advance by loading the front plate with a weight or a uniformly distributed pressure.

The calibration curve thus obtained shall be corrected by means of the above-mentioned expression before it is applied to the case where the pressure cell is arranged in the rigid wall, in contact with the elastic medium.

Pressure cell b (fig. 2).

In this case the pressure distribution is obtained by superposing the loading cases shown in figs. 4a and 4b. (The change in the thickness of the front plate is assumed to be negligible). The deflexion curve for the front plate is determined by the loading case in fig. 4b, assuming here that tensile stresses can be transferred from the elastic medium to the rigid wall, including front plate. In the final condition, where the pressure distribution in the two cases is superposed, there must be no tension anywhere between the elastic medium and the rigid wall, including front plate. For the loading case shown in fig. 4b, the following conditions can be established:

$q_A + q_B = q_o$ at any point within the area F

$w_A = w_B$ " " " " " " " ",

where q_A is the pressure distribution over the area F of the pressure cell, q_B is the change in the stress distribution acting on the surface of the compressible medium within the same area F, w_A is the deflexion of the pressure cell at an arbitrary point under the influence of the stress distribution q_A; and w_B is the deflexion of the compressible medium at the same point, under the influence of the stress distribution q_B.

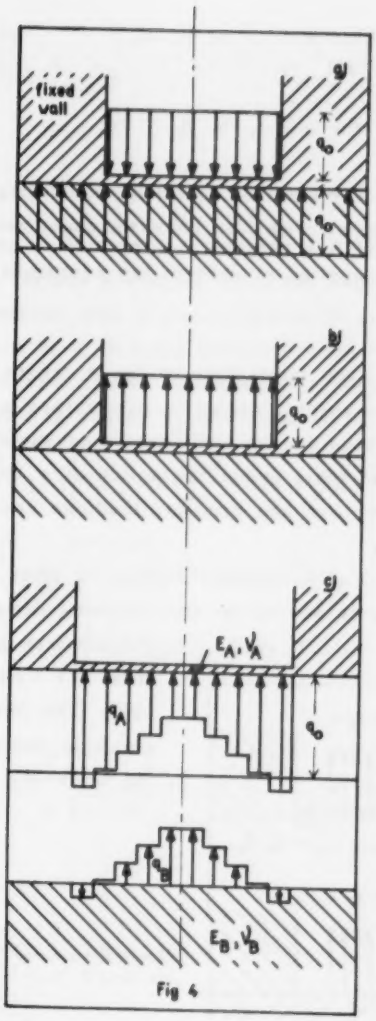

Fig 4

The problem is solved approximately with a stress distribution following a step curve, as shown in fig. 4c, and the conditions are then:

$$q_{An} + q_{Bn} = q_o \quad \text{for } n = 1,\ 3,\ 5,\ 7,\ 9$$

and

$$w_{An} = w_{Bn} \qquad \text{for } n = 1,\ 3,\ 5,\ 7,\ 9.$$

This results in a system of equations consisting of five inhomogeneous linear equations with five unknown quantities.

ΔP is the load applied to deform the compressible medium, i.e. $\Delta P = \int_F q_B dF$.

The deflexion of the front plate of the pressure cell under the action of the stepped loading shown is determined by superposition of the deflexions caused by the individual ring-shaped loadings. The deflexion of the front plate under the action of a ring-shaped loading is found by subtraction of two circular loadings having the same load intensity.

Under the action of a circular loading, a plate that is rigidly fixed along the edge is subject to the following deflexions, using the designations given in fig. 5 (see, for example, (3) page 196). The deflexions are small in comparison with the thickness of the plate.

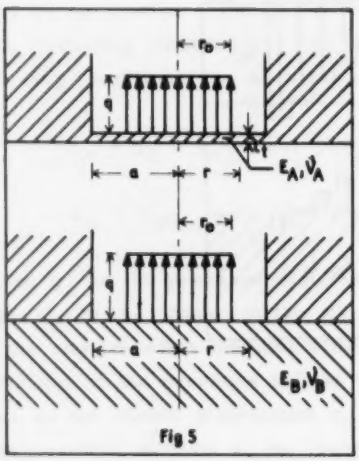

Fig 5

$$w_r = \frac{3(1-\nu_A^2)}{16 \cdot E_A \cdot t^3} \cdot q \cdot r_o^2 \left[4a^2 - (8r^2 + 4r_o^2) \ln\frac{a}{r_o} - \frac{2r^2 r_o^2}{a^2} + \frac{r^4}{r_o^2} - 3r_o^2 \right]$$

for $r \leq r_o$

$$w_r = \frac{3(1-\nu_A^2)}{16 \cdot E_A \cdot t^3} \cdot q \cdot r_o^2 \left[4a^2 - (8r^2 + 4r_o^2) \ln\frac{a}{r} - \frac{2r^2 r_o^2}{a^2} - 4r^2 + 2r_o^2 \right]$$

for $r \geq r_o$.

In table 1, the deflexions for circular and ring-shaped loadings are calculated at various distances from the centre.

An elastic medium with a plane surface in contact with a rigid wall in which there is a circular hole will have the following deflexions within the area of the hole (see (4)) when the load is a circular loading having radius r_o and intensity q (see fig. 5).

$$w_r = \frac{4(1-\nu_B^2)}{\pi \cdot E_B} \cdot q \cdot r \left[E(\frac{r_o}{r}) - E(\frac{r}{a}, \frac{r_o}{r}) - (1-(\frac{r_o}{r})^2)(K(\frac{r_o}{r}) - F(\frac{r}{a}, \frac{r_o}{r})) + \right.$$

$$\left. (1 - \sqrt{1-(\frac{r_o}{a})^2}) \cdot \sqrt{(\frac{a}{r})^2 - 1} \right] \text{ for } a \geq r \geq r_o$$

$$w_r = \frac{4(1-\nu_B^2)}{\pi \cdot E_B} \cdot q \cdot r \left[\frac{r_o}{r} E(\frac{r}{r_o}) - \frac{r_o}{r} E(\frac{r_o}{a}, \frac{r}{r_o}) + \sqrt{(\frac{a}{r})^2 - 1} \cdot (1 - \sqrt{1-(\frac{r_o}{a})^2}) \right]$$

for $r_o \geq r \geq o$.

Here, $E(b, k) = \int_o^b \frac{\sqrt{1-k^2x^2}}{\sqrt{1-x^2}} dx$ for $b \leq 1$, is an elliptical integral of the second kind.

$$E(k) = E(1, k)$$

$$F(a, k) = \int_o^a \frac{dx}{\sqrt{1-x^2}\sqrt{1-k^2x^2}}$$

$$K = F(1, k)$$

These expressions are given in (4) and are calculated in (1) for various values of r and r_o, and the numerical values are transferred direct to table 2 below, which also shows the deflexions for ring-shaped loadings.

Table 1

r_o	r_1	r_2	$\frac{16 E_A \cdot t^3}{3(1-\nu_A^2) a^4 \cdot q} \cdot w$																				$\frac{16 E_A \cdot t^3}{3(1-\nu_A^2) a^4 \cdot q} \cdot w_{av}$ over the ring-shaped area
			r=0		r=0,1·a		r=0,2·a		0,3a		0,4a		0,5a		0,6a		0,7a		0,8a		0,9a		
0,2·a	0	0,2a	0,145	0,145	0,140	0,140	0,126	0,126	0,106	0,106	0,084	0,084	0,062	0,062	0,042	0,042	0,025	0,025	0,012	0,012	0,003	0,003	0,039
	0,2a	0,4a		0,324		0,315		0,296		0,261		0,215		0,164		0,111		0,066		0,031		0,010	0,099
0,4·a			0,469		0,455		0,422		0,367		0,299		0,226		0,153		0,091		0,043		0,013		
	0,4a	0,6a		0,316		0,313		0,295		0,269		0,234		0,188		0,137		0,084		0,042		0,010	0,111
0,6·a			0,785		0,768		0,717		0,636		0,533		0,414		0,290		0,175		0,085		0,023		
	0,6a	0,8a		0,181		0,178		0,172		0,163		0,145		0,125		0,100		0,072		0,035		0,010	0,076
0,8·a			0,966		0,946		0,889		0,799		0,678		0,539		0,390		0,247		0,120		0,033		
	0,8a	1,0a		0,034		0,034		0,033		0,029		0,028		0,024		0,020		0,013		0,010		0,003	0,014
1,0·a			1,000		0,980		0,922		0,828		0,706		0,561		0,410		0,260		0,130		0,036		

Table 2

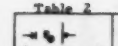 r_o	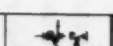 r_1 | r_2		$\frac{s \cdot E_B}{4(1-\nu_B^2)a \cdot q} w$ r=0		r=0, 1a		r=0, 2a		0, 3a		0, 4a		0, 5a		0, 6a		0, 7a		0, 8a		0, 9a		$\frac{s \cdot E_B}{4(1-\nu_B^2)a \cdot q} w_{av}$ over the ring-shaped area
0, 2a	0	0, 2a	0, 294	0, 294	0, 273	0, 273	0, 180	0, 180	0, 091	0, 091	0, 061	0, 061	0, 043	0, 043	0, 032	0, 032	0, 023	0, 023	0, 016	0, 016	0, 010	0, 010	0, 040
	0, 2a	0, 4a		0, 253		0, 264		0, 325		0, 354		0, 256		0, 151		0, 105		0, 075		0, 052		0, 032	0, 116
0, 4a			0, 547		0, 537		0, 505		0, 445		0, 317		0, 194		0, 137		0, 098		0, 068		0, 042		
	0, 4a	0, 6a		0, 209		0, 212		0, 223		0, 246		0, 319		0, 358		0, 263		0, 154		0, 101		0, 060	0, 174
0, 6a			0, 756		0, 750		0, 728		0, 691		0, 635		0, 552		0, 400		0, 252		0, 169		0, 102		
	0, 6a	0, 8a		0, 159		0, 160		0, 164		0, 172		0, 186		0, 212		0, 287		0, 328		0, 231		0, 110	0, 201
0, 8a			0, 915		0, 909		0, 893		0, 864		0, 822		0, 764		0, 687		0, 579		0, 400		0, 213		
	0, 8a	1, 0a		0, 085		0, 086		0, 087		0, 090		0, 095		0, 102		0, 113		0, 136		0, 200		0, 223	0, 152
1, 0a			1, 000		0, 995		0, 980		0, 954		0, 917		0, 866		0, 800		0, 715		0, 600		0, 436		

$q_{An} = q_o - q_{Bn}$.

Therefore:

$$w_{A1} = \frac{3(1-\nu_A^2)a^4 \cdot q_o}{16 \cdot E_A \cdot t^3}\left(0.980 - \frac{q_{B1}}{q_o} \cdot 0.140 - \frac{q_{B3}}{q_o} \cdot 0.315 - \frac{q_{B5}}{q_o} \cdot 0.313 - \frac{q_{B7}}{q_o} \cdot 0.178 - \frac{q_{B9}}{q_o} \cdot 0.034\right)$$

w_{A3} = - " - (0.828 0.106 0.261 0.269 0.163 0.029)

w_{A5} = - " - (0.563 0.062 0.164 0.188 0.125 0.024)

w_{A7} = - " - (0.260 0.025 0.066 0.084 0.072 0.013)

w_{A9} = - " - (0.036 0.003 0.010 0.010 0.010 0.003)

and

$$w_{B1} = \frac{4(1-\nu_B^2)a \cdot q_o}{\pi \cdot E_B}\left(\frac{q_{B1}}{q_o} \cdot 0.273 + \frac{q_{B3}}{q_o} \cdot 0.264 + \frac{q_{B5}}{q_o} \cdot 0.212 + \frac{q_{B7}}{q_o} \cdot 0.160 + \frac{q_{B9}}{q_o} \cdot 0.086\right)$$

w_{B3} = - " - (0.091 0.354 0.246 0.172 0.090)

w_{B5} = - " - (0.043 0.151 0.358 0.212 0.102)

w_{B7} = - " - (0.023 0.075 0.154 0.328 0.136)

w_{B9} = - " - (0.010 0.032 0.060 0.110 0.223)

The system of equations $w_{An} = w_{Bn}$ (n = 1, 3, 5, 7 and 9) is solved for $A = \frac{3\pi}{64}\frac{(1-\nu_A^2)}{(1-\nu_B^2)} \cdot \frac{a^3}{t^3} \cdot \frac{E_B}{E_A}$ = 3, 1, 1/3, 1/10. The results are shown in table 3.

The deflexions w_B shown in table 4 correspond to these values of q.

As a check on the accuracy of the approximation used, a comparison of w_{Bn} and w_{An} can be made at a number of points selected at random. Here, a less accurate check is made, w_{Bn} and w_{An} (for A = 1/10 and 3) being compared for n = 0, 2, 4, 6 and 8, which is not a random distribution. The ratio $\frac{w_{An}}{w_{Bn}}$ shows here an average deviation from 1,00

Table 3

$A = \frac{3\pi}{64}\frac{(1-\nu_A^2)}{(1-\nu_B^2)}\cdot\frac{a^3}{t^3}\cdot\frac{E_B}{E_A}$	$\frac{q_{B_1}}{q_o}$	$\frac{q_{B_3}}{q_o}$	$\frac{q_{B_5}}{q_o}$	$\frac{q_{B_7}}{q_o}$	$\frac{q_{B_9}}{q_o}$	$\frac{\Delta P}{P} = \frac{\int_F q_B dF}{\int_F q_o dF}$
3	1, 068	0, 971	0, 768	0, 394	-0, 365	0, 27
1	0, 796	0, 683	0, 462	0, 117	-0, 219	0, 16
1/3	0, 413	0, 344	0, 215	0, 046	-0, 104	0, 077
1/10	0, 151	0, 126	0, 075	0, 013	-0, 034	0, 028

Table 4

A	$\frac{\pi \cdot E_B}{4(1-\nu_B^2)\cdot a\cdot q_o} w_{B_n}$											
	n=0	n=1	n=2	n=3	n=4	n=5	n=6	n=7	n=8	n=9	n=10	average over the area
3	0, 737	0, 728	0, 697	0, 649	0, 581	0, 495	0, 384	0, 266	0, 142	0, 040	0	0, 294
1	0, 503	0, 495	0, 468	0, 428	0, 372	0, 305	0, 228	0, 149	0, 078	0, 022	0	0, 182
1/3	0, 252	0, 248	0, 233	0, 211	0, 181	0, 146	0, 107	0, 069	0, 036	0, 010	0	0, 087
1/10	0, 091	0, 090	0, 084	0, 076	0, 065	0, 052	0, 038	0, 024	0, 013	0, 004	0	0, 031

of a few per cent. From this it is concluded that the pressure distribution given in table 3 deviates so little from the correct distribution that even in the correct case for $A > 2$, tension must be transferred from the front plate to the elastic medium over part of the area of the pressure cell if contact is to be maintained ($\frac{q_B}{q_o} > 1$). This is at variance with our assumptions so it must be assumed that $A < 2$. A check calculation will show that in the loading cases in question there is compression everywhere between the elastic medium and the rigid wall outside the front plate of the pressure cell. However, A-values higher than 2 are used below; as will be seen later, these values be-

come actual when there is fluid pressure behind the front plate of the pressure cell.

For this type of pressure cell, when the measurement is based on w_{max}, the following is obtained:

$$\frac{dP}{dw}_{w=o} \sim \frac{\Delta P}{w_{(w=o)}} = \frac{0.028 \cdot \pi a^2 q_o}{0.091 \frac{4(1-\nu_B^2) \cdot a \cdot q_o}{\pi \cdot E_B}} \sim 0.8 \cdot \frac{E_B \cdot a}{1-\nu_B^2} \quad \text{for } A = 1/10$$

(see tables 3 and 4)

and

$$\frac{dP}{dw}_{w=o} \sim 0.9 \cdot \frac{E_B \cdot a}{1-\nu_B^2} \quad \text{for } A = 3.$$

When the measurement is based on $w_{average}$, where $w_{av.}$ is the average deflexion over the area of the pressure cell, the following is obtained:

$$\frac{dP}{dw}_{w=o} \sim 2.2 \cdot \frac{E_B \cdot a}{1-\nu_B^2} \quad \text{for } A = 1/10$$

and

$$\frac{dP}{dw}_{w=o} \sim 2.3 \cdot \frac{E_B \cdot a}{1-\nu_B^2} \quad \text{for } A = 3.$$

These are favourable values compared with the corresponding value for pressure cell a, since they can be construed to mean that a relatively large deflexion of the centre of the pressure cell results in only a slight change in the total load acting on the pressure cell.

The signal measured is, however, not uniquely connected with the total load acting on the pressure cell, as was the case for cell a, but is dependent on the distribution of the pressure over the area of the cell.

Here, attention is drawn to the fact that, in practice, pressure cells are frequently calibrated by subjecting the front plate to a uniformly distributed load (fluid pressure) that can be produced in a simple way. The state of deformation of the pressure cell and thereby

also the registered value under the calibration condition (uniformly distributed pressure q_o) may deviate considerably from the state where the cell is placed in a rigid wall and the pressure between the cell and the elastic medium is characterized by being uniformly distributed q_o in the imaginary state in which the deflexion w_r of the front plate is 0 everywhere.

For a fluid pressure q_o over the entire front plate, the following deflexions are obtained:

$$w_{max} = \frac{3(1-\nu_A^2)}{16E_A \cdot t^3} \cdot a^4 \cdot q_o$$

and

$$w_{average} = \frac{3(1-\nu_A^2)}{16E_A \cdot t^3} \cdot a^4 \cdot 0,337 \cdot q_o$$

If the pressure cell is placed in a rigid wall in contact with a compressible medium, and if the pressure between the cell and the medium, when uniformly distributed, has the value q_o, (when $w_r = 0$), the deflexions will be as shown in table 4. w_{max} is found in the column n = 0.

The ratio between the deflexions in the measuring condition (pressure cell placed in the wall in contact with the compressible medium) given in table 4, and the deflexions under the calibration conditions, given by the above-mentioned expressions, can be seen

Table 5

A	Ratio between w_{max} (w_{av}) under operating conditions (q_o uniformly distributed in the imaginary state where w_r=o) and under conditions of calibration (q_o uniformly distributed fluid pressure).				
	Measurement based on w_{max} q_1=o	Measurement based on w_{av}. $\frac{q_1}{q_o}$=0 β_o	$\frac{q_1}{q_o}$=0,3 $\beta_{o,3}$	$\frac{q_1}{q_o}$=0,6 $\beta_{o,6}$	$\frac{q_1}{q_o}$=0,9 $\beta_{0,9}$
0	1,00	1,00	1,00	1,00	1,00
1/10	0,91	0,91	0,94	0,96	0,99
1/3	0,76	0,77	0,83	0,89	0,97
1	0,50	0,54	0,63	0,75	0,92
3	0,25	0,29	0,37	0,56	0,81

from the first two columns of table 5. q_1 is a counter-pressure behind the front plate and is in this case 0. For measurement based on $w_{average}$, this ratio is called β_o.

In fig. 6, the contents of table 5 are shown graphically.

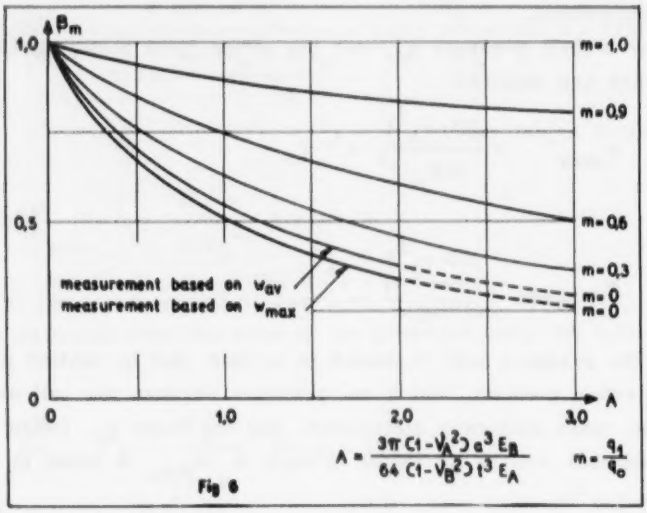

Fig 6

Example:

E_B = 1000 kg/cm^2, which is a commonly applied modulus of elasticity for sand when this is regarded as an elastic medium.

E_A = 2 · 10^6 kg/cm^2, corresponding to the front plate of the pressure cell being made of steel.

$\nu_A \sim \nu_B$

The radius of the front plate a = 50 mm

The thickness of the front plate t = 3 mm.

Thus, $A = \frac{3\pi}{64} \cdot (\frac{50}{3})^3 \cdot \frac{1000}{2 \cdot 10^6} = 0,35$

According to fig. 6, the pressure cell then indicates 75 % of the corresponding calibration value, i.e. the actual pressure is approximately 35 % higher than that measured. The total load on the front plate will in that case be 8 % lower than under the calibration conditions.

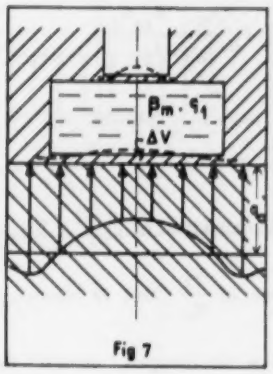

Fig 7

Pressure cells with front plates are often made as shown in fig. 7. Here, the measurements are made on the upper thin plate, the deformation of which may be very considerable, while the deflexions of the front plate are negligible.

For this pressure cell it is assumed that the internal fluid pressure is proportional to ΔV, where ΔV is the volume limited by the two positions of the front plate corresponding to loaded and unloaded condition. The signal measured is proportional to the fluid pressure behind the front plate.

If the pressure cell is calibrated during uniformly distributed, external fluid pressure q_o, the following is obtained:

$$\Delta V_1 = K_1(q_o - q_1),$$

where K_1 is a constant containing E_A, ν_A, t and a, and q_1 is the internal fluid pressure at the loading in question.

The pressure cell is now considered in position in the rigid wall in contact with the elastic medium. The pressure is uniformly distributed q_o in the imaginary state where $w_r = 0$. When $\frac{q_1}{q_o} = m$, the internal fluid pressure has a value that can be denoted $\beta_m \cdot q_1$. By applying the same considerations as used in connexion with figs. 4a and 4b, it will be seen that with this internal fluid pressure, the deflexion curve for the front plate corresponds to that for the loading shown in fig. 4b, with a uniformly distributed counter-pressure $\beta_m q_1$ over the area of the front plate superposed.

This condition will thus give:

$$\Delta V_2 = K_2(q_o - \beta_m q_1),$$

where K_2 is a constant containing E_A, ν_A, E_B, ν_B, t and a.

We now have

$$\frac{\beta_m q_1}{q_1} = \frac{\Delta V_2}{\Delta V_1} = \frac{K_2(q_o - \beta_m q_1)}{K_1(q_o - q_1)} = \beta_o \frac{q_o - \beta_m q_1}{q_o - q_1} ,$$

where β_o is obtained from table 5.

We now have

$$\beta_m = \beta_o \frac{q_o - \beta_m q_1}{q_o - q_1} \quad \text{for the determination of } \beta_m,\ 0 \leq q_1 \leq q_o.$$

β_m is shown in table 5 for various values of $\frac{q_1}{q_o}$ and is shown graphically in fig. 6.

As the shape of the deflexion curve is unchanged, it will be seen that $\frac{dP}{dw}$ remains unaltered when there is internal counter-pressure.

The value for A at which there is pressure everywhere between the pressure cell and the compressible medium depends on the size of q_1 and increases with this. For $\frac{q_1}{q_o} \sim 0.1$, this value is approximately 10.

Pressure cell c (fig. 3)

This type of pressure cell is filled with a fluid. ΔV is assumed to be proportional to q_1, where q_1 is the fluid pressure behind the membrane. This cell registers the load transmitted through the membrane.

We will find $\frac{dP}{dw}_{average}$

According to (4), the deflexion w_r in the loading case shown in fig. 8 is expressed by

$$w_r = \frac{4(1 - \nu_B^2)}{\pi \cdot E_B} \cdot q_o \cdot a \sqrt{1 - \left(\frac{r}{a}\right)^2}$$

If a pressure cell of this type is now arranged in a rigid wall in contact with a compressible medium, where the pressure is uniformly distributed q_o over the area of the cell in the imaginary condition in which the deflexions of the membrane are 0 everywhere, the deflexions of the membrane will be determined by the loading condition shown in fig. 8, superposed by a counter-pressure q_1, which is the fluid pres-

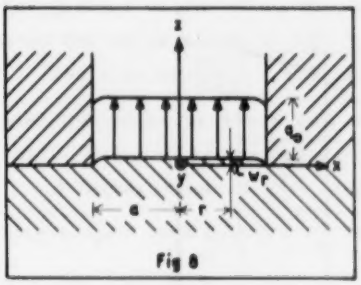

Fig 8

sure behind the membrane. As the deflexions w_r are small, this counter-pressure can be assumed to act in the direction of the Z-axis, so that

$$\Delta P = (q_o - q_1) \cdot \pi a^2, \text{ so that}$$

$$w_{max} = \frac{4}{\pi} \frac{(1-\nu_B^2)(q_o - q_1) \cdot a}{E_B}$$

$$w_{average} = \frac{8}{3\pi} \frac{(1-\nu_B^2)(q_o - q_1) \cdot a}{E_B}$$

and

$$\frac{dP}{dw}_{av.\ w=o} = \frac{\Delta P}{w_{av.}} = 3.7 \cdot \frac{E_B \cdot a}{1-\nu_B^2}$$

A pressure cell of this type can be calibrated by subjecting the membrane to a uniformly distributed load (fluid pressure). The deviation of the calibration condition from the corresponding condition in which the pressure cell is placed in a rigid wall can be expressed by $\frac{dP}{dw}_{av.}$, $w_{av.}$ being fixed on the basis of the knowledge of the design of the cell and of the material constants in question. ΔP can then be determined.

Axially symmetrical pressure distribution under the pressure cell

Pressure cell a (fig. 1)

Fig. 9 shows the relationship between ΔP and w when the pressure under the piston is uniformly distributed (for w = 0). This curve is transferred from (2). For an axially symmetrical load, $\frac{dP}{dw}_{w=o}$ can, in principle, be determined as stated in (1). However, it is hardly necessary to go over the individual loading cases that might arise. If there is pressure over the entire pressure cell for w = 0 and if the pressure gradient at the edge of the pressure cell is not extremely large (figs. 10a and b), $\frac{dP}{dw}_{w=o} \sim 6.1 \cdot \frac{E_B \cdot a}{1-\nu_B^2}$ is obtained, i.e. as in the case of

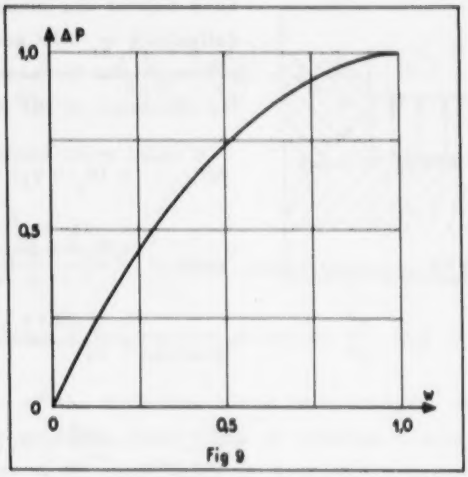

Fig 9

uniformly distributed load. This is seen as follows. If the piston is pulled slightly back, ΔP will be the load required to deform the elastic medium in such a way that contact (i.e. pressure) is obtained everywhere between the elastic medium and the piston except for a narrow ring-shaped area along the edge of the piston. Acting on this ring-shaped area is a pressure that can be reckoned to be uniformly distributed when the pressure gradient (for w = o) is not extremely large and when w is small. The shape of the deflexion curve for this value of w will therefore be almost the same as if there had originally been uniformly distributed pressure over the pressure cell, with a value corresponding to the average stress over the narrow, ring-shaped area. This means that $\frac{\Delta P}{w}$ is also almost the same in the two cases and thus,

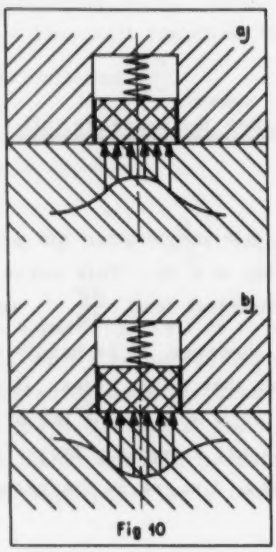

Fig 10

$$\frac{dP}{dw}_{w=o} \sim 6.1 \cdot \frac{E_B \cdot a}{1 - \nu_B^2} .$$

For greater values of w, the ΔP-w curve may deviate considerably from the curve shown in fig. 9.

The size of $\frac{dP}{dw}_{w=0}$ will change when there is no longer pressure over the entire pressure cell for w = 0. Such a state of loading is hardly likely to be encountered very often.

A higher value of $\frac{dP}{dw}_{w=0}$ occurs when there is pressure over a ring-shaped area between r_o and a. As r_o approaches a, $\frac{dP}{dw}_{w=0}$ will increase infinitely.

In order to estimate the value of $\frac{dP}{dw}_{w=0}$ for various values of r_o, the assumption is made here that

$$\frac{\frac{dP}{dw}_{w=0}}{\frac{P}{w}_{max}} = \text{Constant}$$

for a ring-shaped loading between r_o and a, where $0 \leq r_o < a$. The results are shown in tables 6 and 7.

Table 6

 r_o	$\frac{s \cdot E_B}{4(1-\nu_B^2)a \cdot q} \cdot w$											
	r = 0	r=0, 1a	r=0, 2a	0, 3a	0, 4a	0, 5a	0, 6a	0, 7a	0, 8a	0, 9a	max	average over the area
0	1, 000	0, 995	0, 980	0, 954	0, 917	0, 866	0, 800	0, 715	0, 600	0, 436	1, 00	0, 67
0, 2a	0, 706	0, 722	0, 800	0, 863	0, 856	0, 823	0, 768	0, 692	0, 584	0, 426	0, 87	0, 64
0, 4a	0, 453	0, 458	0, 475	0, 509	0, 600	0, 672	0, 663	0, 617	0, 532	0, 394	0, 68	0, 53
0, 6a	0, 244	0, 246	0, 252	0, 263	0, 281	0, 314	0, 400	0, 464	0, 431	0, 334	0, 46	0, 35
0, 8a	0, 085	0, 086	0, 087	0, 090	0, 095	0, 102	0, 113	0, 136	0, 200	0, 223	0, 23	0, 15

It will be seen that with the above assumption, a ring-shaped loading over the area between r_o = 0.8a and a will increase the error by 50 % in comparison with the condition where the loading is uniformly distributed over the entire area of the pressure cell. It will mean, for example, that the error becomes 6 % instead of 4 %.

Table 7

 r_o	$\frac{dP}{dw_{w=o}} \cdot \frac{(1-\nu_B^2)}{E_B \cdot a}$
0	6,1
0,2a	6,7
0,4a	7,5
0,6a	8,5
0,8a	9,5

Pressure cell b (fig. 2)

It has already been stated in the section, "Uniformly distributed pressure under the pressure cell", that the deflexion of the front plate may change the pressure distribution considerably from the original, uniformly distributed pressure. Assuming that there is still pressure everywhere between the cell and the elastic medium, for an axially symmetrical distribution, w_{max} and $w_{average}$ can be found in much the same way as described in the previous section.

However, here we will only consider the conditions for a pressure cell that is very rigid, that is, with a low A-value, so that the rearrangement of the pressure distribution under the cell is negligible. This rearrangement is neglected.

If we then consider the same ring loadings as given in table 7, although with the difference that the total load acting on the cell is the same in all cases, we obtain the results shown in table 8 (based on the figures in table 1).

As expected, the pressure cell is thus seen to be sentisive to deviations from the uniform pressure distribution, for example, for $r_o = 0.4a$, only 70 % of the actual load P (based on measurement of $w_{average}$) will be registered.

Table 8

r_o	q	$\frac{16\,E_A \cdot t^3}{N(1-\nu_A^2)a^4 \cdot q} \cdot w$ r=0, 1a	r=0, 3a	r=0, 5a	0, 7a	0, 9a	max	average over the area	$\frac{w_{mid}}{w_{av}}$
0	q_o	0, 980	0, 828	0, 563	0, 260	0, 036	1, 00	0, 336	1, 00
0, 2a	$\frac{q_o}{0,96}$	0, 875	0, 752	0, 522	0, 245	0, 034	0, 89	0, 310	0, 92
0, 4a	$\frac{q_o}{0,84}$	0, 625	0, 550	0, 401	0, 201	0, 027	0, 64	0, 237	0, 70
0, 6a	$\frac{q_o}{0,64}$	0, 331	0, 300	0, 233	0, 133	0, 020	0, 34	0, 140	0, 42
0, 8a	$\frac{q_o}{0,36}$	0, 095	0, 081	0, 067	0, 036	0, 008	0, 10	0, 040	0, 12

If the load were concentrated on the central part of the plate

$\frac{w_{av}}{w_{av_{r_o=o}}}$ would be greater than 1.

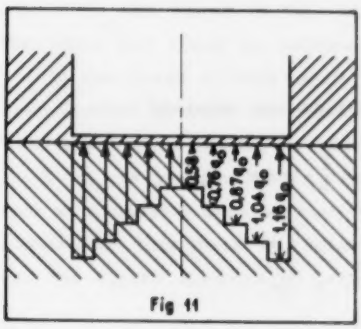

Fig 11

If the pressure distribution in the imaginary state where $w_{r=o}$, is as shown in fig. 11, where the load on the front plate is $\pi a^2 q_o$, the pressure cell, with measurement based on w_{max}, will show 83% of the value that the uniformly distributed pressure q_o would give. If the measurement is based on w_{av}, the corresponding figure will be 86%.

Pressure cell c (fig. 3)

As before, ΔV is proportional to q_1, where q_1 is the fluid pressure behind the membrane. In the imaginary state where $w_r = o$ a total load P acts under the pressure cell. If P is uniformly distributed with the pressure q_o, and if the fluid pressure behind the membrane is $q_1 = \alpha \cdot q_o$, an average deflexion of the membrane is obtained.

$$w_{1_{av}} = \frac{4(1-\nu_B^2)\cdot a}{\pi E_B} \cdot \frac{2}{3}(1-\alpha)q_o$$

If the pressure distribution under the pressure cell is changed to an axially symmetrical loading q_r, so that the total force in the imaginary state where $w_r = o$ is still P, and if, as previously, contact is required between the rigid wall and the compressible medium, the fluid pressure behind the membrane will be changed to $\gamma \cdot \alpha \cdot q_o$. The pressure distribution q_r is approximated with ring-loadings for which deflexions are given in table 2. The average deflexion for q_r can thus be expressed by

$w_{av} = \frac{4(1-\nu_B^2)\cdot a}{\pi \cdot E_B} \cdot C \cdot q_o$, where C is a constant that is found on the basis of the figures in table 2.

Thus; in all, the following equations are obtained:

$$w_{2_{av}} = \frac{4(1-\nu_B^2)\cdot a}{\pi \cdot E_B} \cdot (C \cdot q_o - \frac{2}{3} \cdot \gamma \cdot \alpha \cdot q_o)$$

and

$$\gamma = \frac{w_{2_{av}}}{w_{1_{av}}} = \frac{C - \frac{2}{3} \cdot \gamma \cdot \alpha}{\frac{2}{3}(1-\alpha)} = \frac{3C}{2}$$

Here, γ is found for the same ring-shaped loadings as are used for pressure cells a and b. The results are given in table 9.

If the cell registered correctly, γ should equal 1 for all loading cases. It will be seen, however, that this is not the case.

Table 9

 r_o | q	Y	B	C
0	q_o	1,00	0,67	0,67
0,2a	$\frac{q_o}{0,96}$	0,98	–	0,65
0,4a	$\frac{q_o}{0,84}$	0,92	–	0,62
0,6a	$\frac{q_o}{0,74}$	0,82	–	0,55
0,8a	$\frac{q_o}{0,36}$	0,63	–	0,42

This pressure cell is considerably more sensitive to deviations from the uniformly distributed load than is type a, but is considerably more favourable than type b. If the load P is uniformly distributed over the ring-shaped area from $r_o = 0.4a$ to $r_o = a$, a load is registered that is 8 % lower than if P had been uniformly distributed over the entire area. With the pressure distribution in the imaginary state where $w_r = o$, shown in fig. 11, the pressure cell will show 96 % of the value that would be obtained with uniformly distributed pressure q_o.

In the cases already dealt with for pressure cell c, there has been contact between the rigid wall and the elastic medium. This is not, however, a matter of course, since it is not the case when $\alpha \cdot Y \cdot q_o$ is greater than q_r for $r = a$. Here, there would not be contact in a narrow zone around the edge of the pressure cell. The assumption that there is contact everywhere between the rigid wall and the elastic medium is presumably a reasonable approximation.

Arbitrary pressure distribution under the pressure cell

If the state of pressure under the cell is characterized by $q_{r\theta}$, where $q_{r\theta}$ is the pressure at a point with the polar coordinates r and θ, and there is contact everywhere between the rigid wall and the elastic medium, as far as pressure cell c (fig. 3) is concerned, w_{av} is the same as for an axially symmetrical loading q_r.

where $\int_{\Delta F} q_r \, dF = \int_{\Delta F} q_{r\theta} \, dF$ for any concentric ring-shaped area ΔF.

If contact is lacking between the rigid wall and the elastic medium along a part of the edge of the hole, the conditions will change, but the assumption that there is contact everywhere between the rigid wall and the elastic medium is presumably a reasonable approximation.

If the pressure cell b (fig. 2) is so rigid that it is possible to neglect the change in the state of pressure under the cell, it will at once be seen that w_{av} is the same for arbitrary pressure distribution $q_{r\theta}$ as for the corresponding axially symmetrical distribution q_r. As a consequence of this it will be seen that a state of pressure that increases linearly along the x-axis (fig. 2) and that is independent of the y-position corresponds to a uniformly distributed load. From this it is assumed that the same is the case for any pressure cell of type b, just as it is assumed that $\frac{dP}{dw}_{w=o}$ for pressure cell a (fig. 1) is the same in the two cases. The action of an arbitrary pressure distribution can now be discussed on the basis of the foregoing section.

The pressure cell arranged in the rigid wall, so that it lies near the edge or corner of this.

The compressible medium is semi-infinite. The dimensions of the rigid wall are large in relation to those of the pressure cell.

Pressure cell a

On the basis of the results in (4) it can be concluded that the change caused in the state of pressure by a slight pulling back of the piston is very local, so that $\frac{dP}{dw}_{w=o}$, for the pressure cell placed near the edge of the rigid wall, will only differ slightly from $\frac{dP}{dw}_{w=o}$ for the cell a long way from the edge, when the pressure distribution (for w=o) is the same in the two cases. It can be proved, moreover, that $\frac{dP}{dw}_{w=o}$ for the pressure cell placed near the edge is smaller than or equal to $\frac{dP}{dw}_{w=o}$ for the cell placed a long way from the edge.

Pressure cells b and c

The above can also be expected to apply to these pressure cells.

Friction between the elastic medium and the rigid wall, including pressure cell

In the foregoing we assumed that there was no friction between the elastic medium and the rigid wall plus pressure cell. The condition where the surface of the elastic medium is fixed against horizontal movements is the other limit. Boussinesq has found the following expression for the deflexions of the free surface of a single force acting on a semi-infinite elastic medium:

$$w_1 = \frac{P(1-\nu_B^2)}{\pi E_B} \cdot \frac{1}{r}$$

r is the distance from the force to the point on the surface at which the deflexion is measured.

$$w_2 = \frac{P}{4\pi E_B} \frac{(1+\nu_B)(3-4\nu_B)}{1-\nu_B} \frac{1}{r}$$

The former expression was used as the basis for the foregoing. The latter expression is applied when the surface is fixed against horizontal movements.

The ratio between w_1 and w_2 is the same as between $w_{frictionless}$ and w_{fixed} in the loading cases previously mentioned.

$\frac{w_{fixed}}{w_{frictionless}}$ is dependent on ν_B, as shown in table 10.

Table 10

ν_B	$\frac{w_{fixed}}{w_{frictionless}}$
0	0,75
0,1	0,80
0,2	0,86
0,3	0,92
0,4	0,97
0,5	1,00

Pressure cell a

If the surface of the elastic medium is completely fixed against horizontal movements, which is an upper limit, it can be seen from the above-mentioned table that $\nu_B = 0.1$ (which is a very small value for Poisson's ratio) corresponds to a change in the error shown by the pressure cell of 20 %, so that for example, a cell shows 5 % too little when the surface is frictionless and 6 % too little when the surface is fixed against horizontal movements.

Pressure cells b and c

Here too the case where the surface is fixed against horizontal movements will be an upper limit for the cases occurring in practice. Especially a rubber membrane would be incapable of keeping the surface fixed, so that there we can only have the surface fixed under the rigid wall.

Model test

A test has been made by means of the model technique described in (2) to verify the results given in the above, i.e. in the section "Arbitrary pressure distribution under the pressure cell" and "Pressure cell placed in a rigid wall so that it lies near the edge or corner of this".

The tests shown in figs. 12a, b and c have been carried out. The arrangement shown in fig. 12a corresponds to a problem solved by Boussinesq (rigid, circular piston pressed against semi-infinite elastic medium), although here we are working with finite dimensions of the elastic medium, which results in a smaller deviation from the correct case, as given in (2).

The test (fig. 12a) is made to determine the order of magnitude of the modulus of elasticity, to investigate whether Hooke's law applies in the loading range used, and to establish variations in the modulus of elasticity in the testing period. Poisson's ratio is not determined in this test, but it is found in (2) for the corresponding

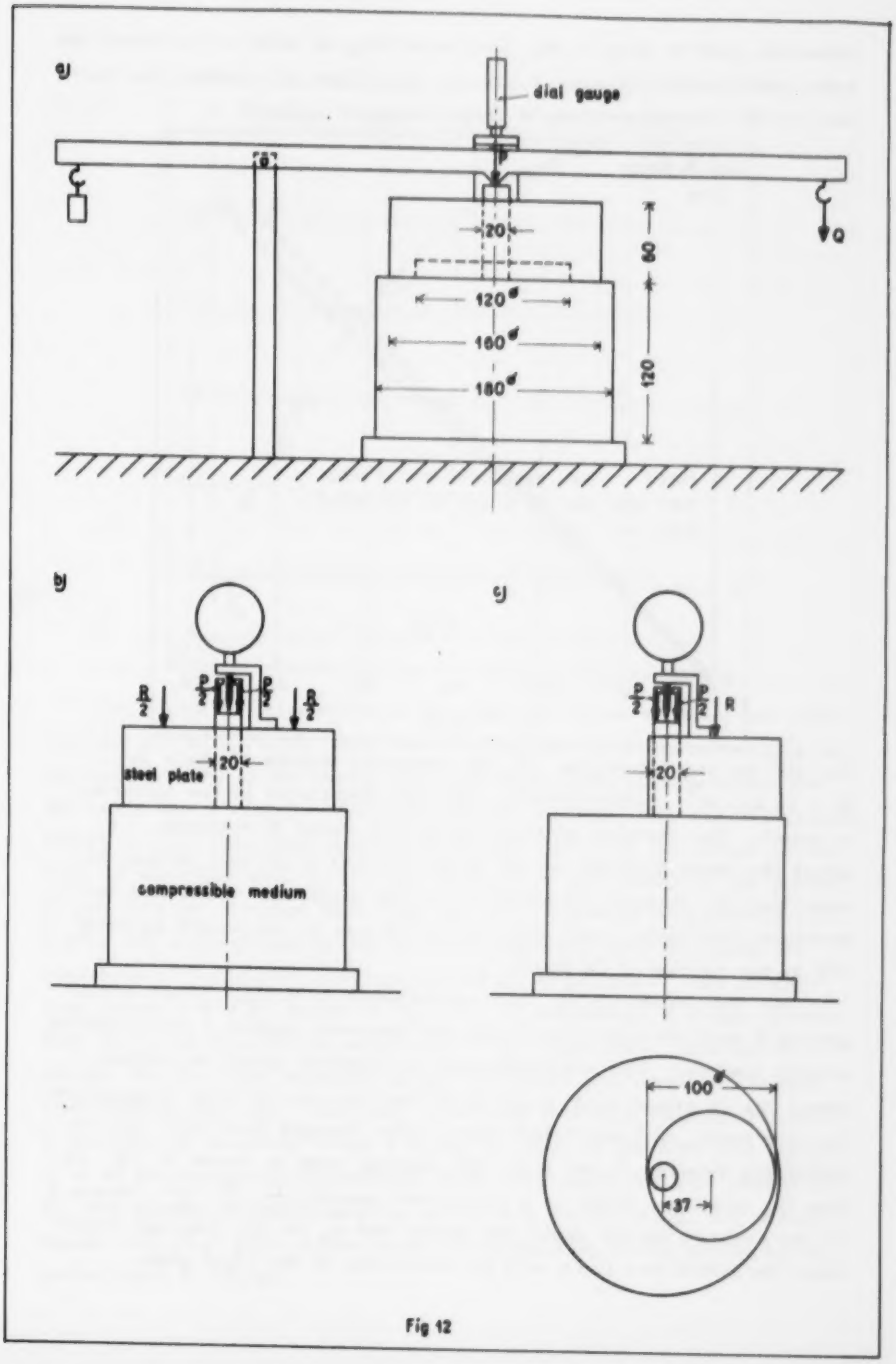
a)
dial gauge
P
Q
20
120
160
180
50
120
b)
R/2
P/2
P/2
R/2
steel plate
20
compressible medium
c)
P/2
P/2
R
20
100
37

Fig 12

material, and is about 0.48, i.e. according to table 10 we obtain the same relationship between P and w, regardless of whether the surface of the elastic medium is frictionless or is fixed.

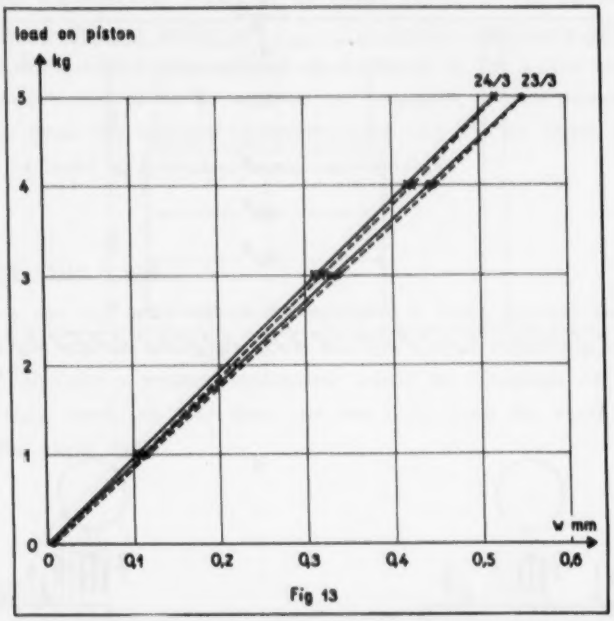

Fig 13

As will be seen from fig. 13, the material follows Hooke's law, $E \sim 55\ kg/cm^2$, rather closely, and the hysteresis of the material is small. The duration of these tests was about 30 minutes, i.e. about the same duration as for tests 12b and c. It will further be seen that the modulus of elasticity of the material, which was determined both before and after tests 12b and c, increased by about 5 % in the course of 24 hours.

The test shown in fig. 12b corresponds to a rigid piston arranged in a semi-infinite, rigid wall and pressed against a semi-infinite elastic medium. The rearrangement of stresses about the piston when this is drawn back is so local that the use of finite dimensions, as used here, will not entail measurable changes (see (2)). The relationship between P and w in this loading case is shown in fig. 14. Use is, however, made of a coordinate system $\frac{q}{q_0}$, $\frac{w}{a} \cdot \frac{1}{q_0}$, where q is the average stress under the piston and q_0 is this average stress when the piston lies flush with the underside of the rigid plate.

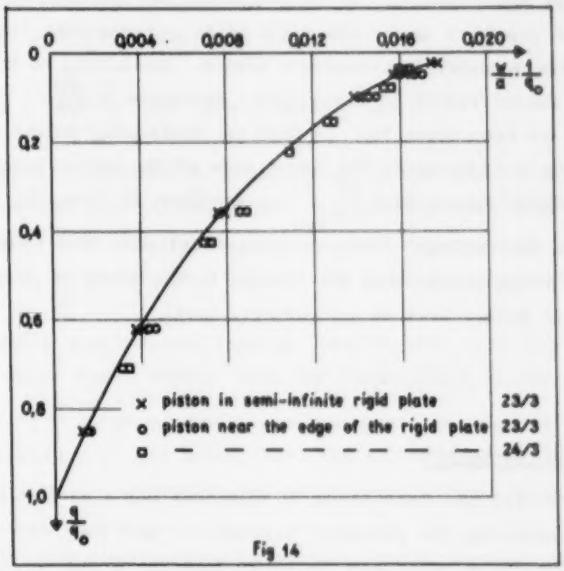

Fig 14

The curve is determined as the average curve between two tests carried out on 23. 3. 60. Only that part of the curve corresponding to the pulling back of the piston has been taken into consideration. On the same day a test (on the same elastic medium) was carried out as shown in fig. 12c. The distance from the centre of the piston to the edge of the rigid wall is 1. 3· R, where R is the radius of the piston. It can also be assumed here that the rearrangement of pressure following the pulling back of the piston is so local that the finite dimensions of the elastic medium are of no importance. The measuring points are also shown in fig. 14. At unloading, a crack formation was seen around the periphery of the rigid plate, and for this reason the test was repeated on 24. 3. 60 after one layer of the elastic medium had been removed. This test was thus carried out with a modulus of elasticity about 5 % greater than in the test with which it is to be compared. Corrections have been made for this change in E, and the corrected measuring points are shown in fig. 14. Here again, only that part of the curve corresponding to the piston being pulled back is shown.

In this test it is a case of a combined action of pressure gradient over the pressure cell and action from the nearby edge, since the state of pressure under the rigid plate corresponds fairly closely to the pressure under Boussinesq's piston. According to the foregoing, the action should result in a negligible decrease in $\frac{dP}{dw}$.

It will be seen from fig. 14 that all measuring points for the case fig. 12c are transposed to the same side of the curve from the case fig. 12b, which means that $\frac{dP}{dw}_{w=o}$ is smallest in case fig. 12c. This agrees with the findings of the previous sections. The difference is not large, which means that the change in the state of pressure when the piston is pulled back is exceedingly local.

Resumé and conclusion

An appraisal has been made of different types of pressure cells used for measuring the pressure between a rigid wall and an elastic medium. The three types are shown in figs. 1, 2 and 3, and are characterized by the front plate being designed as a rigid piston, a plate fixed along the edge, and a membrane with fluid pressure behind it, respectively.

The three types are investigated on the basis of the following cases:

1. Uniformly distributed pressure under the pressure cell.
2. Axially symmetrical pressure distribution under the pressure cell.
3. Arbitrary pressure distribution under the pressure cell.
4. The pressure cell arranged in the rigid wall so that it lies near the edge or corner of this.

Further, a model test corresponding to a combination of loading cases 3 and 4 has been carried out on the type of pressure cell shown in fig. 1.

Pressure cell a (fig. 1)

The relationship between the load on the piston and the pulling back of the piston is expressed as

$$\frac{dP}{dw}_{w=o} = 6.1 \cdot \frac{E_B \cdot a}{1-\nu_B^2} \quad \text{for case 1 (see(1) and (2)).}$$

The signal measured is proportional to the load on the piston. This means that this pressure cell can be calibrated with weights, and that the calibration curve thus obtained can be used provided a correction is made for the action of the pulling back of the piston expressed by $\frac{dP}{dw}$.

An axially symmetrical loading (case 2) will only alter the ratio $\frac{dP}{dw}_{w=o}$ in those cases where, with the piston fixed in the position w=o, there is a very large pressure gradient near the edge of the piston or when pressure is not acting over the entire area of the pressure cell. Such states of pressure are very seldom likely to occur in practice.

A uniformly distributed ring-shaped loading between r = 0.8a and r = a is an example of such an extreme loading. For this, $\frac{dP}{dw}_{w=o} \sim 9.5 \cdot \frac{E_B \cdot a}{1-\nu_B^2}$, (on the assumption that $\frac{\frac{dP}{dw}_{w=o}}{\frac{P}{w}_{max}}$ = constant). If the error was previously 2 % for a uniformly distributed load over the entire pressure cell (w=o), it will now be about 3 %.

For an arbitrary loading, $\frac{dP}{dw}_{w=o}$ can be expected to equal $\frac{dP}{dw}_{w=o}$ for an axially symmetrical loading formed by this arbitrary loading.

It can further be proved that for a pressure cell placed near the edge of the rigid wall (case 4), $\frac{dP}{dw}_{w=o}$ is less than or equal to $\frac{dP}{dw}_{w=o}$ for a cell placed in a semi-infinite rigid wall, when the pressure distribution over the cell (for w=o) is the same in both cases.

Model tests have confirmed the above-mentioned results (cases 3 and 4). Even though this type of pressure cell has a high value of the ratio $\frac{dP}{dw}_{w=o}$, it seems to be very insensitive to pressure gradients, which is an advantage, since in practice pressure distributions under the piston frequently arise that may deviate considerably from a uniformly distributed loading and that cannot be determined.

Friction between the elastic medium and the rigid wall, including piston, will entail such small changes in comparison with the frictionless connexion that they can usually be neglected.

Pressure cell b (fig. 2)

The ratio $\frac{dP}{dw}_{w=o}$ for case 1 is found here by using an approximation method.

$$\frac{dP}{dw}_{max} \sim 0.8 \cdot \frac{E_B \cdot a}{1-\nu_B^2}$$

$$\frac{dP}{dw}_{average} \sim 2.2 \cdot \frac{E_B \cdot a}{1-\nu_B^2}$$

This type of pressure cell thus has favourable $\frac{dP}{dw}$ - values. The relationship between the load acting on the front plate and the deflexion of the front plate is, however, not unique, which is a disadvantage since it is attempted to determine this load by measurement of w.

It will be seen that the pressure distribution under the pressure cell (for the cells without fluid pressure behind the front plate) may change considerably from the original uniformly distributed load, depending on the dimensions of the front plate and on the physical constants E_A, ν_A, E_B and ν_B.

This means that the calibration conditions must be checked. Thus a not unimportant error may arise if the calibration curve refers to a test in which the front plate of the pressure cell is subjected to a uniformly distributed load (fluid pressure). The dependence of this error on the constant

$$A = \frac{3\pi}{64} \frac{(1-\nu_A^2)}{(1-\nu_B^2)} \cdot \frac{a^3}{t^3} \cdot \frac{E_B}{E_A}$$ is shown in fig. 6.

As appears from fig. 6, this type of pressure cell can be improved by transmitting the pressure on the front plate through a fluid behind the front plate to a thin plate, the deformations of which are measured.

As is already apparent from the foregoing, a pressure cell of this type is sensitive to deviations from the uniformly distributed state of pressure over the entire area of the cell. If the state of pressure under a pressure cell with a very rigid front plate is as shown in fig. 11, the cell will indicate 83 % of the value that would be indicated if the corresponding pressure were uniformly distributed. This value applies when the measurement is based on w_{max}. If the measurement is based on w_{av}, the corresponding value will be 86 %.

Provided there is contact everywhere between the front plate and the compressible medium, an arbitrary loading will give the same results as an axially symmetrical loading produced by the arbitrary loading as stated previously.

When placed near an edge or corner of the rigid wall, this pressure cell must be assumed to act in the same way as cell a, just as friction between the elastic medium and the rigid wall, including cell, must be assumed to bring about corresponding small changes.

Pressure cell c (fig. 3)

For uniformly distributed pressure under the entire pressure cell (case 1),

$$\frac{dP}{dw} = 3.7 \cdot \frac{E_B \cdot a}{1 - \nu_B^2} .$$

The pressure transmitted through the membrane remains uniformly distributed over the surface of the pressure cell with a value that is dependent on w. This cell can therefore be calibrated by loading the membrane with a uniformly distributed load (fluid pressure), and the calibration curve thus obtained can be applied provided a correction is made for the effect of the pulling back, w, by using the expression $\frac{dP}{dw}$.

The recording of this pressure cell is, as was the case for cell b, although not to the same degree, dependent upon the pressure distribution under the membrane (in the imaginary state, w_r=o). The pressure distribution shown in fig. 11 will result in a recording of 96 %

of the value that would be obtained if the same resultant load were uniformly distributed over the entire area of the cell.

It is possible to visualize pressure distributions under the cell that will, like the distribution shown in fig. 10b, prevent contact between the rigid wall and the compressible medium over a narrow zone around the edge of the cell. One of the assumptions forming the basis for the above is thus not fulfilled. Just what effect this will have on the error cannot be ascertained without knowing the pressure distribution, not only under the cell (w_r=o), but also under the rigid wall near the cell. The assumption that there is contact everywhere is presumably a reasonable approximation.

If there is contact between the rigid wall and the elastic medium, an arbitrary pressure distribution (case 3) will give the same result as the axially symmetrical distribution corresponding to the former.

If this pressure cell is placed near an edge or a corner in the rigid wall, the same conditions will presumably apply as for cell a, still on the assumption that there is contact everywhere between the elastic medium and the rigid wall.

Friction can be expected to be of even less importance for this type of pressure cell than for the other two, since the elastic medium under a rubber membrane is not fixed.

If the compressible medium is a material consisting of grains, the grain size must be so small in comparison with the thickness of the membrane that the deflexions of the membrane are negligible between the grains.

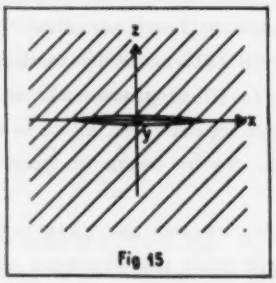

Fig 15

The results reached for cases 1, 2 and 3 (no friction) can, for this pressure cell, easily be transferred to the case where a cell is placed in an infinitely elastic medium, as shown in fig. 15. (There is axial symmetry about the z-axis and the xy-plane is a plane of symmetry). The pressure cell is very thin.

Literature.

1. S. Gravesen: "Elastisk halvrum begrænset af stiv plade med cirkulært stempel", Festskrift til professor Anker Engelund. Meddelelse nr. 10 fra Laboratoriet for Bygningsteknik, 1959.

2. Vagn Askegaard: "The measurement of pressure between an infinitely rigid wall and a compressible medium", Festskrift til professor Anker Engelund, Meddelelse nr. 10 fra Laboratoriet for Bygningsteknik, 1959.

3. Raymond J. Roark: "Formulas for Stress and Strain", 3rd Edition, McGraw-Hill, 1954.

4. S. Gravesen: "Elastic semi-infinite medium bounded by a rigid plate with a circular hole", Bygningsstatiske Meddelelser, nr. 3, 1959.

THE LAST VOLUMES OF ACTA POLYTECHNICA

Civil Engineering and Building Construction Series

(The predecessor of Acta Polytechnica Scandinavica)

Volume 4

Nr 1 LANGE HANSEN, P: *The Plastic Theory of Curved Beams with Compressive Axial Forces.* Acta P 215 (1957), 32 pp, Sw. Kr 5: 00 UDC 624.072.3:539.214

Nr 2 ISAKSSON, Å: *Creep Rates of Excentrically Loaded Test Pieces.* Acta P 219 (1957), 33 pp, Sw. Kr 4: 50 UDC 620.172.251.2

Nr 3 IDORN, G M: *Concrete Deterioration of a Foundation.* Acta P 221 (1957), 48 pp, Sw. Kr 8: 00 UDC 620.163.24:693.5

Nr 4 ORDING, F BOYE: *Die Beständigheit der Basislatten.* Acta P 225 (1957), 16 pp, Sw. Kr 7: 00 UDC 526.25

Nr 5 SUNDSTRÖM, E: *Creep Buchling of Cylindrical Shells.* Acta P 230 (1957), 34 pp, Sw. Kr 5: 00 UDC 539.434:624.074.4-434.1

Nr 6 KUDSK-JØRGENSEN, B: *Calculation of Time-Concentration Curves in a Stationary, Laminar Liquid Flow Through a Circular-Cylindrical Tube.* Acta P 233 (1957), 18 pp, Sw. Kr 5: 00 UDC 532.517.2:612.13

Nr 7 ENGELUND, F: *On the Theory of Multiple-Well Systems.* Acta P 234 (1957), 11 pp, Sw. Kr 5: 00 UDC 551.495.54

Nr 8 BRINCH HANSEN, J: *Calculation of Settlements by Means of Pore Pressure Coefficients.* Acta P 235 (1957), 14 pp, Sw. Kr 5: 00 UDC 624.131.326

Nr 9 DAHL, N J: *On Water Supply from Wells.* Acta P 236 (1957), 17 pp, Sw. Kr 5: 00 UDC 551.49:628.112

Nr 10 LUNDGREN, H: *Dimensional Analysis in Soil Mechanics.* Acta P 237 (1957), 32 pp, Sw. Kr 6: 00 UDC 624.131

ACTA POLYTECHNICA SCANDINAVICA

Civil Engineering and Building Construction Series

Ci 1 BRETTING, A E: *Stable Channels.* (Acta P 245/1958), 130 pp, Sw. Kr 7: 00 UDC 626.01:627.1

Ci 2 OSTERMAN, J: *Notes on the Shearing Resistance of Soft Clays.* (Acta P 263/1959) 24 pp, Sw. Kr. 7.00 UDC 624.131.222

Ci 3 EIDE, OWE AND JOHANNESEN, IVAR J: *Measurement of Strut Loads in the Excavation for Oslo Technical School.* (Acta P 266/1960) 14 pp. Sw. Kr. 7.00 UDC 624.131.532:624.134.4

Ci 4 JOHANNESEN, IVAR J: *Test Section and Installation of Test Equipment, Oslo Subway* and ØIEN KJELL: *An Earth Pressure Cell for use on Sheet Piles* (Acta P 267/1960) 16 pp, Sw. Kr. 7.00 UDC 624.131.386:624.134.4

Ci 5 KJÆRNSLI, BJØRN: *Test results, Oslo Subway* (Acta P. 268/1960) 11 pp. Sw. Kr. 7.00 UDC 624.131.532:624.134.4

Ci 6 KYRKLUND, HARALD: *Über die Einschätzung von Biegespannungen in gekrümmten Balken.* (Acta P. 274/1960) 56 pp. + fig. Sw. Kr. 7: 00 UDC 624.072.7

Ci 7 VUORELAINEN, O: *Thermal Conditions in the Ground from the viewpoint of Foundation Work, Heating and Plumbing Installations and Draining.* (Acta P. 277/1960) 40 pp. Sw. Kr. 7: 00 UDC 624.131.436 + 551.525

Ci 8 VUORELAINEN, O: *The Temperature Field Produced in the Ground by a Heated Slab Laid direct on Ground, and the Heat Flow from Slab to Ground.* (Acta P. 278/1960) 59 pp. Sw. Kr. 7: 00 UDC 536.2:697.133:69.025.1

Ci 9 VUORELAINEN, O: *The Temperatures under Houses Erected Immediately on the Ground and the Heat Losses from their Foundation Slab.* (Acta P. 289/1960) 105 pp. Sw. Kr. 14: 00 UDC 536.2:697.133:69.025.1

Ci 10 GIBSON, R. E. AND LO, K. Y: *A Theory of Consolidation for Soils Exhibiting Secondary Compression.* (Acta P. 296/1961) 16 pp. Sw. Kr 7: 00 UDC 624.131.542:624.131.526

Price Sw. Kr. 7.00